European Radiology (2019) 29:4603–4612
https://doi.org/10.1007/s00330-018-5982-1

COMPUTED TOMOGRAPHY

Single- and dual-energy CT pulmonary angiography using second- and third-generation dual-source CT systems: comparison of radiation dose and image quality

Lukas Lenga[1] · Franziska Trapp[2] · Moritz H. Albrecht[1] · Julian L. Wichmann[1] · Addison A. Johnson[3] · Ibrahim Yel[1] · Tommaso D'Angelo[1,4] · Christian Booz[1] · Thomas J. Vogl[2] · Simon S. Martin[1,3]

Received: 7 September 2018 / Revised: 23 November 2018 / Accepted: 17 December 2018 / Published online: 21 January 2019

Abstract

Objectives To evaluate radiation exposure and image quality in matched patient cohorts for CT pulmonary angiography (CTPA) acquired in single- and dual-energy mode using second- and third-generation dual-source CT (DSCT) systems.

Methods We retrospectively included 200 patients (mean age, 65.5 years ± 15.7 years) with suspected pulmonary embolism—equally divided into four study groups ($n = 50$) and matched by gender and body mass index. CTPA was performed with vendor-predefined second-generation (group A, 100-kV single-energy computed tomography (SECT); group B, 80/Sn140-kV dual-energy computed tomography (DECT)) or third-generation DSCT (group C, 100-kV SECT; group D, 90/Sn150-kV DECT) devices. Radiation metrics were assessed using a normalized scan range of 27.5 cm. For objective image quality evaluation, dose-independent figure-of-merit (FOM) contrast-to-noise ratios (CNRs) were calculated. Subjective image analysis included ratings for overall image quality, reader confidence, and image artifacts using five-point Likert scales.

Results Calculations of the effective dose (ED) of radiation for a normalized scan range of 27.5 cm showed nonsignificant differences between SECT and DECT acquisitions for each scanner generation ($p \geq 0.253$). The mean effective radiation dose was lower for third-generation groups C (1.5 mSv ± 0.8 mSv) and D (1.4 mSv ± 0.7 mSv) compared to second-generation groups A (2.5 mSv ± 0.9 mSv) and B (2.3 mSv ± 0.6 mSv) (both $p \leq 0.013$). FOM-CNR measurements were highest for group D. Qualitative image parameters of overall image quality, reader confidence, and image artifacts showed nonsignificant differences among the four groups ($p \geq 0.162$).

Conclusions Third-generation DSCT systems show lower radiation dose parameters for CTPA compared to second-generation DSCT. DECT can be performed with both scanner generations without radiation dose penalty or detrimental effects on image quality compared to SECT.

Key Points

- *Radiation exposure showed nonsignificant differences between SECT and DECT for both DSCT scanner devices.*
- *Dual-energy CTPA provides equivalent image quality compared to standard image acquisition.*
- *Subjective image quality assessment was similar among the four study groups.*

Keywords Computed tomography angiography · Pulmonary embolism · Radiation dosage · Diagnostic imaging · Thorax

✉ Lukas Lenga
lukas.lenga@gmail.com

[1] Division of Experimental Imaging, Department of Diagnostic and Interventional Radiology, University Hospital Frankfurt, Theodor-Stern-Kai 7, 60590 Frankfurt, Germany

[2] Department of Diagnostic and Interventional Radiology, University Hospital Frankfurt, Frankfurt, Germany

[3] Department of Radiology and Radiological Science, Medical University of South Carolina, Charleston, SC, USA

[4] Department of Biomedical Sciences and Morphological and Functional Imaging, University Hospital Messina, Messina, Italy

Abbreviations

ADMIRE	Advanced modeled iterative reconstruction
ATVS	Automated attenuation-based tube voltage selection
BMI	Body mass index
CNR	Contrast-to-noise ratio
CT	Computed tomography
$CTDI_{vol}$	Volume CT dose index
DECT	Dual-energy computed tomography
DLP	Dose-length product
DSCT	Dual-source computed tomography

ED	Effective dose
FOM	Figure-of-merit
HU	Hounsfield units
ROI	Region of interest
SAFIRE	Sinogram-affirmed iterative reconstruction
SD	Standard deviation
SECT	Single-energy computed tomography

Introduction

Rapid and accurate detection of pulmonary embolism (PE) is crucial, as PE represents a potentially life-threatening disease [1]. Computed tomography pulmonary angiography (CTPA) is the gold standard for the detection of pulmonary clots [1, 2]. However, the proper diagnosis is often challenging due to poor contrast conditions, respiratory motion artifacts, or insufficient cardiac pumping function [3].

Dual-energy CT (DECT) has gained wide acceptance in clinical practice in oncologic as well as vascular imaging as it provides unique post-processing capabilities for functional and quantitative analysis [4, 5]. Low-keV virtual monoenergetic images (VMI+) derived by DECT datasets increase the iodine signal attenuation and improve the detection of incidental PE in staging examinations of the thorax in the portal venous phase [6]. Moreover, the calculation of iodine perfusion maps has been shown to result in an increased diagnostic accuracy for the detection of PE [7].

However, the combination of two X-ray beam energies in DECT examinations led to concerns about additional radiation exposure [8]. To overcome this drawback, recent developments in third-generation dual-source CT (DSCT) systems focused on the implementation of advanced dose-saving technologies. New levels of dual-energy tube voltage combinations, higher X-ray tube current reserves, and a thicker tin filter were installed to keep radiation exposure to a minimum [9]. Previous studies investigating differences in radiation exposure of single-energy CT (SECT) and DECT reported divergent results [8, 10, 11]. Moreover, the radiation dose of single- and dual-energy CTPA using second- or third-generation DSCT scanners has not been evaluated so far.

Thus, the aim of our current study was to compare radiation exposure and image quality in matched patient cohorts for CTPA acquired in single- and dual-energy modes using second- and third-generation DSCT systems.

Materials and methods

Patient population

Our retrospective study received institutional review board approval with a waiver for written informed consent. The targeted query of our local CT database yielded a total of 200 nonconsecutive patients. All patients were clinically suspected of having PE and had undergone CTPA in single- and dual-energy modes on second- or third-generation DSCT devices. Overall, 100 men (mean age, 64.6 ± 13.8; range, 19–85) and 100 women (mean age, 66.9 ± 18.2; range, 27–106) were included in our analysis. Four study groups (A–D) were created with 50 patients in each group (25 men and 25 women in each group). Exclusion criteria of our study consisted of faint contrast conditions in the pulmonary arteries ($n = 23$), motion artifacts ($n = 18$), flow rate less than 4 mL/s ($n = 12$), and imprecise region of interest (ROI) positioning ($n = 11$). In cases with reduced renal function (glomerular filtration rate < 45 mL/min), known allergies to iodinated contrast agent, and age ≤ 18 years, an individual patient preparation protocol was established based on the clinical severity of symptoms. To account for direct comparisons between the study groups, patients were matched by gender and body mass index (BMI; target BMI, 26.5 kg/m^2). All patient data are summarized in Table 1.

At our institution, second-generation DSCT was replaced by third-generation DSCT scanner in April 2015. For both second- and third-generation DSCT systems, vendor-predefined examination protocols in SECT and DECT mode were applied. Our study was designed to accurately evaluate differences in radiation dose between SECT and DECT examinations performed with second- and third-generation DSCT devices. We decided to examine patients in either single-energy or dual-energy technique on the basis of active studies conducted at our institution at the time of the examination.

SECT and DECT image acquisition

Patients in groups A and B had been examined using second-generation DSCT (Somatom Definition Flash, Siemens Healthineers) in SECT (group A) and DECT (group B) mode, respectively. A third-generation DSCT scanner (Somatom Force, Siemens) was used for patients assigned to control groups C (SECT) and D (DECT). Single-energy DSCT was acquired at 100 kV for both scanner generations while tube voltage settings for second- and third-generation dual-energy DSCT systems were 80/Sn140 kV and 90/Sn150 kV, respectively. For both scanner generations, automated tube current modulation (CARE Dose 4D, Siemens Healthineers) was applied. A medium soft tissue convolution kernel was used for second-generation (B26f) and third-generation (Bv40) DSCT data reconstruction. Images were further reconstructed in axial and coronal view with a section thickness of 3 mm and an interslice gap of 1 mm.

CTPA image acquisition was timed using a bolus-tracking technique, placing a circular ROI within the pulmonary trunk. The scan was initiated 7 s after a threshold of 100 Hounsfield units (HU) was reached during shallow inspiratory breath

Table 1 Summary of patient characteristics with ranges in parenthesis

	Group A	Group B	Group C	Group D
Number of patients	50	50	50	50
Male/female	25/25	25/25	25/25	25/25
Age (years)	66.2 ± 15.6 (33–99)	68.2 ± 14.6 (30–97)	64.5 ± 16.9 (31–106)	62.8 ± 15.4 (19–85)
BMI kg/m^2	25.9 ± 2.6 (20.9–32.8)	26.1 ± 3.2 (21.3–33.7)	26.3 ± 3.8 (22.4–35.2)	26.0 ± 3.4 (21.3–32.6)

hold. The scan range for CTPA started at the upper abdomen, covering the thorax up to the cervical root in caudocranial direction. Nonionic contrast agent was administered at a dose of 1.0 mL/kg body weight (400 mg iodine/mL; Imeron, Bracco) with a maximum of 60 mL at a flow rate of 4 mL/s via a superficial antecubital vein followed by a 30-mL saline chaser. Table 2 shows a detailed overview of all CT parameters.

Radiation dose assessment

The following radiation metrics were recorded from the examination protocol: dose-length product (DLP), volume CT dose index ($CTDI_{vol}$), tube current, and acquisition length in centimeters. Effective dose (ED) values were obtained by multiplying the DLP with a chest-specific conversion coefficient (k) of 0.014 [mSv / (mGy × cm)] for SECT and DECT acquisition [12–14]. To allow for a consistent comparison of radiation parameters among the groups, mean scan acquisition length for DLP was set to a standard thoracic CT range of 27.5 cm [12, 14].

Objective image quality assessment

Objective image quality evaluation was performed by a radiologist with 4 years of experience in CTPA imaging, who was responsible for all objective image quality measurements. Signal attenuation and standard deviation (SD) in HU were measured by drawing homogenous ROIs within the pulmonary trunk (ROI size, 60–100 mm^2), the right and left pulmonary arteries (ROI size, 30–80 mm^2), and the ascending aorta (ROI size, 70–120 mm^2). Adjacent anatomical structures, aortic wall calcifications, and areas of focal heterogeneity (e.g., beam-hardening artifacts) were carefully spared. For each anatomical region, repeated measurements were performed to avoid data inaccuracies.

Contrast-to-noise (CNR) calculations included additional ROI measurements within the subcutaneous fat at the level of the tracheal bifurcation (ROI size, 80–120 mm^2) and the erector spinae muscle (ROI size, 80–120 mm^2). Image noise was defined as the SD of fat. The CNR of each anatomical entity (pulmonary trunk, right and left pulmonary arteries,

Table 2 DSCT acquisition parameters

	Group A	Group B	Group C	Group D
Dual-source CT generation	Second-generation	Second-generation	Third-generation	Third-generation
Acquisition mode	SECT	DECT	SECT	DECT
Tube voltage (kV)	100	80/Sn140	100	90/Sn150
Tube current (ref. mAs)	180	180/80	120	60/46
Pitch	0.6	0.6	0.6	0.6
Rotation time (s)	0.5	0.5	0.5	0.5
Collimation	128 mm × 0.6 mm	2 mm × 128 mm × 0.6 mm	192 mm × 0.6 mm	2 mm × 192 mm × 0.6 mm
Section thickness (mm)	3	3	3	3
Iterative reconstruction algorithm	SAFIRE (strength level 3)	SAFIRE (strength level 3)	ADMIRE (strength level 3)	ADMIRE (strength level 3)
Increment (mm)	1	1	1	1
Kernel	B26f	B26f	Bv40	Bv40
Linear blending in dual-energy mode	–	60% ay 80 kV, 40% at Sn140 kV	–	60% at 90 kV, 40% at Sn150 kV
Tin filter	–	Selective photon shield	–	Selective photon shield II

SAFIRE sinogram-affirmed iterative reconstruction

ascending aorta) was calculated by applying the following formula:

$$\mathrm{CNR} = \frac{\mathrm{HU\ (ROI)}-\mathrm{HU\ (muscle)}}{\mathrm{image\ noise}}$$

To account for different tube voltage settings obtained in groups A–D, objective image quality assessment included additional figure-of-merit (FOM) calculations. FOM values were calculated as the ratio of CNR^2 to ED to guarantee for CNR evaluation independent to ED [10, 15].

Subjective image quality evaluation

Three radiologists with 3 years to 4 years of experience in CTPA imaging, who were not involved in objective image quality assessment, evaluated each image series subjectively with regard to overall image quality, image artifacts, and diagnostic confidence. A consensus reading was performed in preset, standard CTPA window settings (width, 800 HU; level, 300 HU). Each reader was allowed to freely modify window settings to their own requirements. Prior to the readout sessions, observers were blinded to clinical data, CT scan protocol, and CT system.

All observers reviewed second- and third-generation SE- and DE-CTPA in random order using five-point Likert scales [16]. Overall image quality (ranging from 1 [poor image quality] to 5 [excellent image quality]), image artifacts (ranging from 1 [major artifacts] to 5 [no artifacts perceivable]), and diagnostic confidence scores (ranging from 1 [examination non-diagnostic] to 5 [high diagnostic confidence]) were recorded.

Statistical analysis

For statistical analysis, commercially available statistic software was used (MedCalc statistical software, version 18.6; MedCalc Software bvba). A p value < 0.05 indicated a statistically significant difference.

Continuous variables were expressed as means ± SD. Medians were applied for variables that did not follow normal distribution. The normality of data distribution was confirmed by using the Kolmogorov-Smirnov test. For normal data distribution, analysis of variance test (ANOVA) was used. In cases of non-Gaussian distribution, the Wilcoxon matched pairs test was applied. The Spearman correlation test was used for assessment of radiation dose among the four study groups, taking the effect of BMI on ED into account.

The intraclass correlation coefficient (ICC) indicated interobserver agreement on subjective image quality parameters. According to previous studies, ICC values of < 0.40 were considered as poor agreement, 0.40–0.59 as fair agreement, 0.60–0.74 as good agreement, and 0.75–1.0 as excellent agreement [17].

The subjective image evaluation further included the assessment of differences in diagnostic image quality among the four study groups. The observers were asked to rank the three subjective image parameters in acceptable and unacceptable diagnostic image quality (unacceptable, scores 1–2; acceptable, scores 3–5). Thus, two variables were generated that were used to differentiate between diagnostic image quality acceptability and unacceptability among the groups. For the dichotomized variables, the chi-square test or Fisher exact test was applied.

Results

Radiation dose evaluation

A detailed record of all radiation dose parameters is summarized in Table 3. A strong and positive correlation between BMI and ED was found in each study group (group A, $r^2 = 0.613$; group B, $r^2 = 0.637$; group C, $r^2 = 0.704$; group D, $r^2 = 0.602$; all $p \leq 0.001$). The corresponding scatter diagrams are illustrated in Fig. 1. Lowest radiation dose values for DLP averaged to a scan length of 27.5 cm were observed in group D. These values had no statistically significant difference with group C ($p = 0.738$) but significantly lower than groups A and B ($p \leq 0.012$).

Group A demonstrated the highest EDs of radiation for a normalized scan length of 27.5 cm with significant differences compared to groups C and D ($p \leq 0.013$), while differences between groups A and B compared to differences between groups C and D were not significantly different ($p \geq 0.253$). Direct comparisons between second-generation (groups A and B) and third-generation (groups C and D) DSCT scanners showed significantly lower radiation exposure for third-generation DSCT ($p \leq 0.001$), while differences between SECT and DECT acquisitions were nonsignificant for each scanner generation ($p \geq 0.631$).

Objective image quality evaluation

The results of objective image quality parameters are listed in Table 4. Highest CNR values for the pulmonary trunk, the right and left pulmonary arteries, and the ascending aorta were consistently found in group D with significant differences compared to groups A and B ($p \leq 0.039$). Differences in CNR calculations between groups C and D did not reach statistical significance ($p \geq 0.441$).

The assessment of dose-independent FOM-CNR calculations for the pulmonary trunk, the right and left pulmonary arteries, and the ascending aorta showed highest values in group D with significant differences compared to groups A

Table 3 Radiation dose values

	Group A	Group B	Group C	Group D	*p* value
$CTDI_{vol}$ (mGy)	6.5 ± 2.3 (3.0–11.0)	6.0 ± 1.6 (3.5–9.5)	3.9 ± 2.1 (0.4–9.8)	3.9 ± 1.9 (1.7–10.0)	Group A vs. B and group C vs. D, $p \geq 0.339$; all other, $p \leq 0.043$
DLP (mGy × cm)	236.0 ± 121.2 (90–729)	202.7 ± 54.0 (118–330)	162.0 ± 137.6 (8.1–669.2)	138.5 ± 135.9 (51.7–767.1)	Group A vs. B and group C vs. D, $p \geq 0.492$; all other, $p \leq 0.049$
Effective dose (mSv)	3.3 ± 1.7 (1.3–10.2)	2.8 ± 0.8 (1.7–4.6)	2.3 ± 1.9 (0.1–9.4)	1.9 ± 1.9 (0.7–10.7)	Group A vs. B and group C vs. D, $p \geq 0.168$; all other, $p \leq 0.012$
Mean acquisition length (cm)	36.5 ± 12.5 (25.9–82.0)	34.1 ± 3.2 (29.3–45.7)	38.1 ± 12.4 (18.4–68.6)	33.0 ± 9.8 (18.0–76.4)	All, $p \geq 0.062$
DLP of 27.5 cm (mGy × cm)	180.0 ± 62.4 (81.7–301.7)	164.4 ± 45.1 (96.3–261.8)	108.4 ± 57.6 (12.1–268.1)	106.2 ± 52.4 (47.6–276.1)	Group A vs. B and group C vs. D, $p \geq 0.346$; all other, $p \leq 0.012$
Effective dose of 27.5 cm (mSv)	2.5 ± 0.9 (1.1–4.2)	2.3 ± 0.6 (1.3–3.7)	1.5 ± 0.8 (0.2–3.8)	1.4 ± 0.7 (0.7–3.9)	Group A vs. B and group C vs. D, $p \geq 0.253$; all other, $p \leq 0.013$

Data are given as mean ± standard deviation and range in parenthesis

and B ($p \leq 0.032$), but nonsignificant in comparison with group C ($p \geq 0.210$). Overall, vessel-related FOM-CNR calculations demonstrated nonsignificant differences between groups A and B ($p \geq 0.069$). Differences in pulmonary trunk measurements in group C were higher than those in group A, but nonsignificant between the two groups ($p = 0.374$). The lowest FOM-CNR values were consistently observed in group A.

Subjective image quality evaluation

All subjective image quality parameters are given in Table 5. When evaluating subjective image parameters regarding overall image quality, all image series were rated as good/excellent. Group D showed highest rating scores for overall image quality (4.3 ± 0.7), while lowest ratings were found in group A (3.5 ± 0.6). Differences between groups A and D were statistically significant ($p \leq 0.027$). All other image series showed nonsignificant differences ($p \geq 0.341$). The assessment of image artifacts and reader confidence also demonstrated consistently good/excellent rating scores for all groups with best ratings for group D (4.1 ± 0.8 and 4.2 ± 0.6, respectively). However, differences between the four groups were not significant ($p \geq 0.162$).

Interrater agreement among the four groups was considered excellent with regard to overall agreement (ICC, 0.89; 95% CI, 0.86–0.91). The detailed analysis on all image parameters—overall image quality (ICC, 0.88; 95% CI, 0.83–0.92), image artifacts (ICC, 0.82, 95% CI, 0.78–0.84), and reader confidence (ICC, 0.88; 95% CI, 0.83–0.91)—was also excellent.

All cases of groups A, C, and D were categorized as acceptable (50/50) by the observers. In group B, one case was considered unacceptable (49/50) due to image artifacts. The observers categorized none of the series as unacceptable due to impaired image quality. No significant differences were found among the four groups ($p \geq 0.648$). Figure 2 illustrates an overview of the different series acquired with the different scan protocols.

Discussion

In this study, we investigated direct differences in image quality and radiation exposure between SECT and DECT acquisitions for routine CTPA protocols using second- and third-generation DSCT scanners. Our results emphasize that DE-CTPA does not increase radiation exposure or affect image quality compared to SECT acquisition for each scanner generation. In fact, we found a significant dose reduction for third-generation DSCT in comparison with second-generation DSCT, while differences between SECT and DECT were nonsignificant for both DSCT systems.

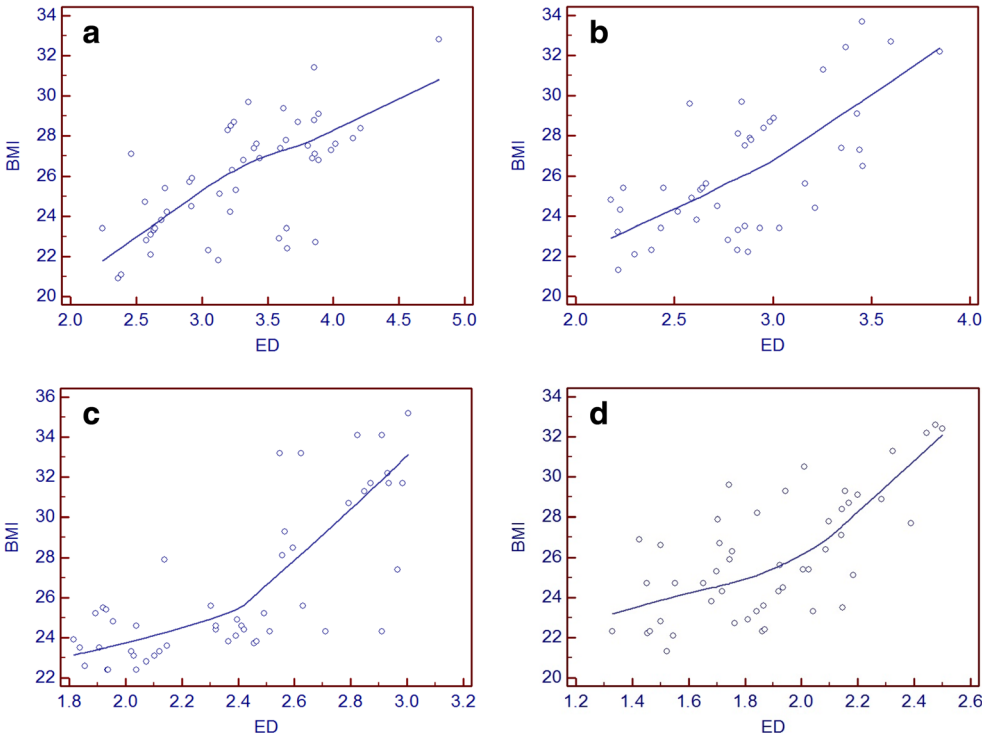

Fig. 1 Scatter diagrams demonstrate a strong and positive correlation between ED and BMI for all study groups (**a** $r^2 = 0.613$; **b** $r^2 = 0.637$; **c** $r^2 = 0.704$; **d** $r^2 = 0.602$; all $p \leq 0.001$)

Moreover, radiation dose reduction for third-generation DSCT did not result in decreased subjective image quality ratings. Dose-independent FOM-CNR measurements are generally considered as an independent predictor of objective image quality. Our investigation revealed highest FOM-CNR values for third-generation DE-CTPA. Hence, CTPA can routinely be performed with both scanner generations in SECT and DECT modes, while DE-CTPA provides several spectral imaging features that may facilitate the detection of embolic clots.

Since the implementation of DECT applications in clinical practice is growing, concerns about increased radiation dose delivered by two X-ray beam sources have been raised. Only few prior studies have investigated direct differences in radiation exposure and image quality between SECT and DECT acquisitions with heterogeneous results [8, 10, 11, 18–20]. Bauer et al [21] performed the only study that compared differences in radiation dose and image quality for SE- and DE-CTPA using first- and second-generation DSCT devices. The authors reported significant radiation dose reduction for second-generation DE-DSCT compared to first-generation SE-DSCT. In a phantom study by Schenzle et al [8], comparable results for radiation exposure were observed between SECT and DECT image series using second-generation DSCT scanners. Few studies have also investigated the effect of radiation dose between SECT and DECT in contrast-enhanced abdominal imaging. While Wichmann et al [10] and De Cecco et al [11] found a small, but significant increase in radiation dose for second-generation abdominal DE-DSCT examinations, results from another study demonstrated similar radiation dose values for SECT and DECT examinations for second- and third-generation DSCT. On the contrary, Schmidt et al [19] found significantly lower radiation dose values for contrast-enhanced DE-DSCT examinations of the abdomen in comparison with SE-DSCT acquisition.

We found the lowest radiation dose values in third-generation DSCT with a nonsignificant difference between SECT and DECT acquisitions. Objective image quality parameters were found to be superior for third-generation DECT. In our opinion, technical advances in third-generation DSCT may have largely influenced our results. Improved tube current capabilities for the low tube voltage spectrum may have led to radiation exposure reduction. For third-generation DSCT devices, new tube voltage combinations for both X-ray tubes were designed that enable kilovolt settings between 70 and 150 kV. A new X-ray tube was installed that increases the maximum power for the low-energy spectrum [9]. This X-ray tube enables examinations to be performed at a peak tube current of 1300 mA. The implementation of these features resulted in an improvement of image quality and reduction of radiation dose [22]. Another technical development in third-generation DSCT included the introduction of the selective photon shield II technique. This technique uses an additional tin filter directly in front of the high- and low-energy X-ray tube that allows for image acquisition with tin filtration in the single-energy mode. Consequently, third-generation DSCT is more dose efficient due to an increased sensitivity to photon flux while

Table 4 Objective image quality parameters

	Group A	Group B	Group C	Group D	*p* value
Contrast-to-noise ratio					
Pulmonary trunk	17.9 ± 10.2 (4.3 ± 51.2)	19.7 ± 7.6 (2.2–31.4)	25.7 ± 16.6 (9.3 ± 62.1)	30.2 ± 23.7 (9.8–135.9)	Group A vs. B, $p = 0.253$; group C vs. D, $p = 0.768$; all other, $p \leq 0.032$
Right pulmonary artery	16.7 ± 9.3 (3.7–43.4)	18.4 ± 8.5 (2.9–40.0)	24.7 ± 15.3 (7.8–56.4)	28.5 ± 22.1 (9.3–126.2)	Group A vs. B $p = 0.288$; group C vs. D, $p = 0.829$; all other, $p \leq 0.035$
Left pulmonary artery	16.4 ± 9.6 (3.9–49.2)	18.2 ± 10.5 (1.7–43.0)	24.2 ± 15.6 (8.2–54.5)	28.7 ± 21.3 (9.5–122.7)	Group A vs. B $p = 0.459$; group C vs. D, $p = 0.839$; all other, $p \leq 0.039$
Ascending aorta	14.3 ± 8.8 (1.3–39.1)	15.3 ± 7.0 (5.0–38.9)	17.9 ± 8.5 (6.1–32.8)	22.5 ± 11.4 (8.7–66.7)	Group A vs. B, $p = 0.315$; group C vs. D, $p = 0.441$; all other, $p \leq 0.029$
Figure-of-merit contrast-to-noise ratio					
Pulmonary trunk	155.6 ± 191.3 (7.7–789.2)	169.8 ± 129.6 (2.3–544.8)	203.6 ± 216.9 (40.5–982.1)	251.4 ± 227.9 (29.2–939.8)	Group A vs. B, $p = 0.192$; group A vs. C, $p = 0.374$; group C vs. D, $p = 0.515$; all other, $p \leq 0.001$
Right pulmonary artery	133.9 ± 157.0 (5.7–568.3)	155.2 ± 146.2 (2.6–606.1)	194.4 ± 142.6 (28.3–605.3)	229.8 ± 122.5 (26.9–521.0)	Group A vs. B $p = 0.069$; group C vs. D, $p = 0.891$; all other, $p \leq 0.002$
Left pulmonary artery	129.9 ± 167.2 (6.5 ± 730.0)	151.8 ± 155.6 (1.3–602.4)	190.7 ± 132.6 (29.5–529.2)	234.5 ± 181.2 (27.9–659.3)	Group A vs. B, $p = 0.459$; group C vs. D, $p = 0.210$; all other, $p \leq 0.016$
Ascending aorta	106.8 ± 135.6 (0.7–529.3)	114.1 ± 144.2 (7.8–741.6)	153.4 ± 175.2 (18.8–747.4)	186.6 ± 163.5 (18.5–802.3)	Group A vs. B, $p = 0.339$; group C vs. D, $p = 0.441$; all other, $p \leq 0.032$

Data are given as mean ± standard deviation and range in parenthesis

simultaneously reducing image noise [23]. Based on these developments, we believe that differences in radiation dose and image quality between second- and third-generation DSCT systems could be translated into other anatomical regions and imaging protocols, such as unenhanced chest CT examinations.

In our study, increased FOM-CNR values were observed for the third-generation DSCT system. Several factors impact image quality and CNR during image acquisition which can generally be divided into acquisition and reconstruction parameters. A potential explanation for increased FOM-CNR at third-generation DSCT may be the new iterative reconstruction algorithm (advanced modeled iterative reconstruction (ADMIRE)). Multiple studies have reported reduced radiation exposure and improved image quality for ADMIRE in comparison with second-generation iterative reconstruction algorithm SAFIRE [24, 25]. In addition, a new medium smooth filter kernel became available for third-generation DSCT. This may also attribute to the improved objective image parameters for third-generation DSCT (Bv40) in relation to second-generation DSCT (B26f). Nevertheless, the improved objective image quality parameters did not result in superior rating scores for subjective image quality rating. We performed vendor-predefined SE-CTPA examinations at 100-kVp for second- and third-generation DSCT scanners. Additional radiation dose-saving techniques can be achieved by applying automated attenuation-based tube voltage selection (ATVS) that is only available for SECT image acquisition. It has been shown that in most cases, the selected tube voltage at third-generation DSCT body angiography is lower in comparison with second-generation DSCT ATVS [26]. For DECT acquisition, further potential radiation exposure reduction techniques include the calculation of virtual nonenhanced images and patient-specific spectral separation on the basis of patient size and habitus [9, 27].

Some limitations of our study have to be considered. First, due to the fact that we conducted a retrospective study, the decision to perform CTPA in either SECT or DECT mode was made according to inclusion criteria of ongoing institutional studies at the time of the examination. Second, because of subsequent patient enrollment, potential selection bias might be present. Third, as DECT datasets show a characteristic FOV, blinding of the observers during subjective image reading remains challenging. We therefore performed four reading sessions, each session containing randomly selected images of second- and third-generation scanners in SECT and DECT mode. Sufficient time intervals (at least two weeks) between the reading sessions were employed to enhance blinding. Our results demonstrated nonsignificant differences for subjective image parameters between the four groups; hence, the influence of DECT-FOV configurations might be marginal. In addition, we only evaluated images with 3 mm section thickness. Results for objective and subjective image analysis may vary

Table 5 Subjective image quality parameters

	Group A	Group B	Group C	Group D	*p* value
Overall image quality	3.5 ± 0.6 (2–4)	4.1 ± 0.6 (2–5)	3.7 ± 0.6 (3–5)	4.3 ± 0.7 (3–5)	Group A vs. D, $p \leq 0.027$; all other, $p \geq 0.341$
Image artifacts	3.6 ± 0.7 (2–4)	4.0 ± 0.7 (2–5)	3.8 ± 0.6 (3–5)	4.1 ± 0.8 (3–5)	All groups, $p \geq 0.162$
Reader confidence	3.7 ± 0.6 (1–4)	3.9 ± 0.9 (3–5)	4.0 ± 0.7 (3–5)	4.2 ± 0.6 (3–5)	All groups, $p \geq 0.224$

Data are given as mean ± standard deviation and range in parenthesis

in thin collimation images. Fourth, although investigations on diagnostic accuracy were not performed, subjective image quality evaluation comprised ratings of diagnostic confidence. Fifth, as we used fixed examination protocols recommended and predefined by the vendors, additional dose-saving techniques were not considered. New iterative reconstruction algorithms in third-generation technology may also have contributed to radiation dose reduction and image quality improvement, as well as the application of ATVS in SECT imaging [25, 28]. Sixth, ED estimations are subject to high inaccuracies. This is mainly based on the fact that ED is a derived parameter which depends on various factors. ED estimates do not allow risk stratification of ionizing radiation for each individual as interindividual factors such as age are not represented. Nevertheless, dose estimation in CT using the ED is recommended by the "European Working Group for Guidelines on Quality Criteria in CT" as it is supposed to be practical and allows for comparison of different radiological exposures (e.g., CT, radiography) [29]. To date, no organ-specific conversion factor has been developed for ED

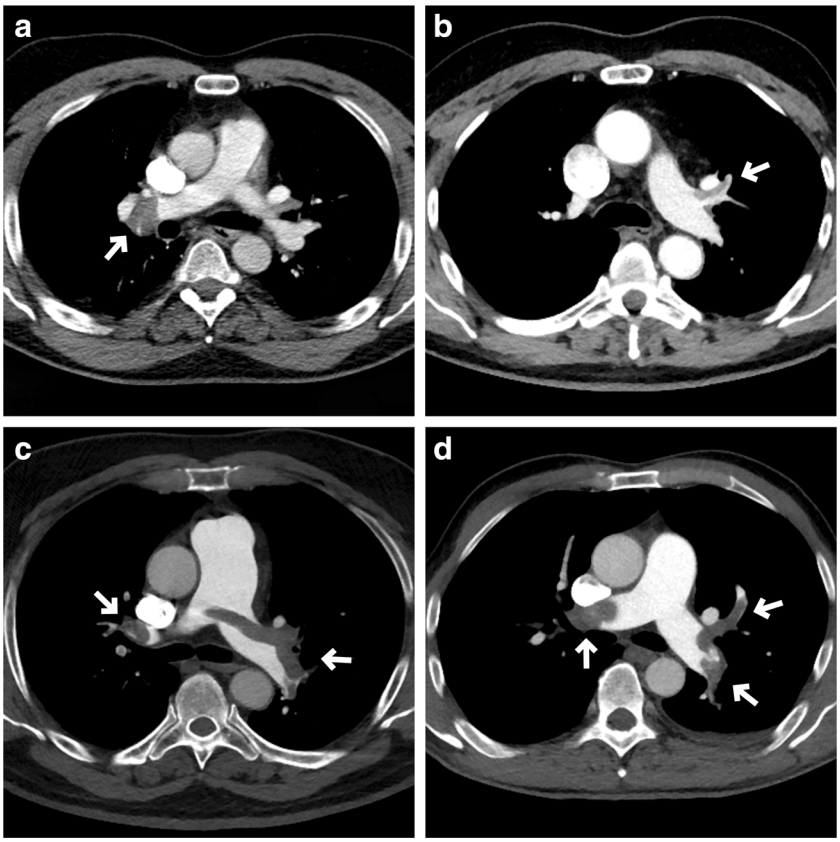

Fig. 2 Examinations performed with second-generation (**a**, **b**) and third-generation (**c**, **d**) DSCT scanners in single-energy (**a**, **c**) or dual-energy (**b**, **d**) modes show pulmonary emboli (*arrows*). Image of a 57-year-old male patient with PE in the right pulmonary artery (**a**) performed with a second-generation DSCT scanner in single-energy mode at 100 kV (3.2 mSv). The medical history of the patient revealed recurrent deep leg vein thrombosis. Second-generation DECT image of a 70-year-old male patient with pulmonary clot of the left upper lobe pulmonary artery (**b**) after a long-distance flight (2.9 mSv). Image acquisition was obtained at 80/Sn140 kV. A 59-year-old male patient with history of cancer of unknown primary (CUP) showed distinct bilateral PE (**c**). Images were acquired at 100 kV using third-generation DSCT in single-energy mode (2.4 mSv). Third-generation DECT images (1.8 mSv) obtained of a 45-year-old male patient with histologically proven seminoma demonstrate PE in the right and left pulmonary arteries (**d**). DE-CTPA was performed at 90/Sn150 kV

estimation in DECT examinations. In accordance with prior studies investigating radiation exposure at DECT, we have also used organ-specific weighting factors derived from SECT studies [10, 12]. As the organ-specific conversion coefficient substantially impacts ED estimations, developing such coefficients for DECT examinations is crucial to account for potential differences between single-energy and dual-energy technologies. Finally, our findings solely pertain to DSCT imaging. Other dual-energy technologies such as rapid kilovolt switching and dual-layer detector systems were not investigated.

In conclusion, our results emphasize that CTPA with vendor-predefined examination protocols can routinely be performed in SECT and DECT modes on second- and third-generation DSCT devices without radiation dose penalty, while third-generation DSCT is more dose efficient. Dual-energy CTPA provides equivalent or greater image quality and is dose-neutral when compared to standard image acquisition for both DSCT platforms, while providing enhanced capabilities for functional and quantitative analysis.

Funding The authors state that this work has not received any funding.

Compliance with ethical standards

Guarantor The scientific guarantor of this publication is Lukas Lenga.

Conflict of interest The authors of this manuscript declare relationships with the following companies: Julian L. Wichmann received speakers' fees from GE Healthcare and Siemens Healthcare. Moritz H. Albrecht received speakers' fees from Siemens Healthcare. However, all other authors report no potential conflict of interest. Data was controlled by authors with no potential conflict of interest.

Statistics and biometry No complex statistical methods were necessary for this paper.

Informed consent Written informed consent was waived by the institutional review board.

Ethical approval Institutional review board approval was obtained.

Methodology
- retrospective
- cross-sectional study
- performed at one institution

References

1. Torbicki A, Perrier A, Konstantinides S et al (2008) Guidelines on the diagnosis and management of acute pulmonary embolism: the Task Force for the Diagnosis and Management of Acute Pulmonary Embolism of the European Society of Cardiology (ESC). Eur Heart J 29:2276–2315
2. Stein PD, Fowler SE, Goodman LR et al (2006) Multidetector computed tomography for acute pulmonary embolism. N Engl J Med 354:2317–2327
3. Wittram C, Maher MM, Yoo AJ, Kalra MK, Shepard JA, McLoud TC (2004) CT angiography of pulmonary embolism: diagnostic criteria and causes of misdiagnosis. Radiographics 24:1219–1238
4. Albrecht MH, Trommer J, Wichmann JL et al (2016) Comprehensive comparison of virtual monoenergetic and linearly blended reconstruction techniques in third-generation dual-source dual-energy computed tomography angiography of the thorax and abdomen. Invest Radiol 51:582–590
5. Beeres M, Trommer J, Frellesen C et al (2016) Evaluation of different keV-settings in dual-energy CT angiography of the aorta using advanced image-based virtual monoenergetic imaging. Int J Cardiovasc Imaging 32:137–144
6. Weiss J, Notohamiprodjo M, Bongers M et al (2017) Effect of noise-optimized monoenergetic postprocessing on diagnostic accuracy for detecting incidental pulmonary embolism in portal-venous phase dual-energy computed tomography. Invest Radiol 52:142–147
7. Leithner D, Wichmann JL, Vogl TJ et al (2017) Virtual monoenergetic imaging and iodine perfusion maps improve diagnostic accuracy of dual-energy computed tomography pulmonary angiography with suboptimal contrast attenuation. Invest Radiol 52:659–665
8. Schenzle JC, Sommer WH, Neumaier K et al (2010) Dual energy CT of the chest: how about the dose? Invest Radiol 45:347–353
9. Krauss B, Grant KL, Schmidt BT, Flohr TG (2015) The importance of spectral separation: an assessment of dual-energy spectral separation for quantitative ability and dose efficiency. Invest Radiol 50:114–118
10. Wichmann JL, Hardie AD, Schoepf UJ et al (2017) Single- and dual-energy CT of the abdomen: comparison of radiation dose and image quality of 2nd and 3rd generation dual-source CT. Eur Radiol 27:642–650
11. De Cecco CN, Darnell A, Macías N et al (2013) Second-generation dual-energy computed tomography of the abdomen: radiation dose comparison with 64- and 128-row single-energy acquisition. J Comput Assist Tomogr 37:543–546
12. Shrimpton PC, Hillier MC, Lewis MA, Dunn M (2006) National survey of doses from CT in the UK: 2003. Br J Radiol 79:968–980
13. (2007) The 2007 recommendations of the International Commission on Radiological Protection. ICRP publication 103. Ann ICRP 37:1–332
14. Christner JA, Kofler JM, McCollough CH (2010) Estimating effective dose for CT using dose-length product compared with using organ doses: consequences of adopting International Commission on Radiological Protection publication 103 or dual-energy scanning. AJR Am J Roentgenol 194:881–889
15. Schindera ST, Nelson RC, Mukundan S Jr et al (2008) Hypervascular liver tumors: low tube voltage, high tube current multi-detector row CT for enhanced detection–phantom study. Radiology 246:125–132
16. Sullivan GM, Artino AR Jr (2013) Analyzing and interpreting data from likert-type scales. J Grad Med Educ 5:541–542
17. Cicchetti DV (1994) Guidelines, criteria, and rules of thumb for evaluating normed and standardized assessment instruments in psychology. Psychol Assess 6:284–290
18. Mahmood U, Horvat N, Horvat JV et al (2018) Rapid switching kVp dual energy CT: value of reconstructed dual energy CT images and organ dose assessment in multiphasic liver CT exams. Eur J Radiol 102:102–108

19. Schmidt D, Söderberg M, Nilsson M, Lindvall H, Christoffersen C, Leander P (2018) Evaluation of image quality and radiation dose of abdominal dual-energy CT. Acta Radiol 59:845–852
20. Primak AN, Giraldo JC, Eusemann CD et al (2010) Dual-source dual-energy CT with additional tin filtration: dose and image quality evaluation in phantoms and in vivo. AJR Am J Roentgenol 195: 1164–1174
21. Bauer RW, Kramer S, Renker M et al (2011) Dose and image quality at CT pulmonary angiography-comparison of first and second generation dual-energy CT and 64-slice CT. Eur Radiol 21: 2139–2147
22. Meyer M, Haubenreisser H, Schoepf UJ et al (2014) Closing in on the K edge: coronary CT angiography at 100, 80, and 70 kV-initial comparison of a second- versus a third-generation dual-source CT system. Radiology 273:373–382
23. Gordic S, Morsbach F, Schmidt B et al (2014) Ultralow-dose chest computed tomography for pulmonary nodule detection: first performance evaluation of single energy scanning with spectral shaping. Invest Radiol 49:465–473
24. Nam SB, Jeong DW, Choo KS et al (2017) Image quality of CT angiography in young children with congenital heart disease: a comparison between the sinogram-affirmed iterative reconstruction (SAFIRE) and advanced modelled iterative reconstruction (ADMIRE) algorithms. Clin Radiol 72:1060–1065
25. Schmid AI, Uder M, Lell MM (2017) Reaching for better image quality and lower radiation dose in head and neck CT: advanced modeled and sinogram-affirmed iterative reconstruction in combination with tube voltage adaptation. Dentomaxillofac Radiol 46: 20160131
26. Winklehner A, Gordic S, Lauk E et al (2015) Automated attenuation-based tube voltage selection for body CTA: performance evaluation of 192-slice dual-source CT. Eur Radiol 25: 2346–2353
27. Graser A, Johnson TR, Hecht EM et al (2009) Dual-energy CT in patients suspected of having renal masses: can virtual nonenhanced images replace true nonenhanced images? Radiology 252:433–440
28. Mangold S, De Cecco CN, Wichmann JL et al (2016) Effect of automated tube voltage selection, integrated circuit detector and advanced iterative reconstruction on radiation dose and image quality of 3rd generation dual-source aortic CT angiography: an intra-individual comparison. Eur J Radiol 85:972–978
29. Mayo-Smith WW, Hara AK, Mahesh M, Sahani DV, Pavlicek W (2014) How I do it: managing radiation dose in CT. Radiology 273: 657–672